International Journal of Heat and Mass Transfer 55 (2012) 4688–4700

Contents lists available at SciVerse ScienceDirect

International Journal of Heat and Mass Transfer

journal homepage: www.elsevier.com/locate/ijhmt

Indirect heating strategy for laser induced hyperthermia: An advanced thermal model

Leonid A. Dombrovsky [a,*], Victoria Timchenko [b], Michael Jackson [c]

[a] Joint Institute for High Temperatures, Krasnokazarmennaya 17A, NCHMT, Moscow 111116, Russia
[b] School of Mechanical and Manufacturing Engineering, University of New South Wales, Sydney 2052, Australia
[c] Department of Radiation Oncology, Prince of Wales Hospital, NSW, Sydney 2031, Australia

ARTICLE INFO

Article history:
Received 14 March 2012
Received in revised form 12 April 2012
Accepted 13 April 2012
Available online 15 May 2012

Keywords:
Cancer
Hyperthermia
Laser heating
Gold nanoshells
Absorption and scattering
Transient thermal model

ABSTRACT

A novel heating strategy based on laser irradiation of surrounding tissues as an alternative to direct irradiation of superficial tumors is proposed and analyzed for the first time. The computational analysis is based on two-dimensional axisymmetric models for both radiative transfer and transient heat transfer in the human body. A diffuse component of the radiation field is calculated using P_1 approximation. Coupled transient energy equations and kinetic equations for composite human tissue take into account the metabolic heat generation and heat conduction, blood perfusion through capillaries, the volumetric heat transfer between arterial blood and tissue, the thermal conversions in blood and tumor tissue, the periodic laser heating, and also heat exchange between a human body and ambient medium. An example problem for a superficial human cancer has been solved numerically to illustrate the relative role of the problem parameters on the transient temperature field during hyperthermia treatment. In particular, the effect of embedded gold nanoshells which strongly absorb the laser radiation is analyzed. It is shown that required parameters of tumor hyperthermia can be also reached without gold nanoshells.

1. Introduction

The use of laser light directly or via minimally invasive fiber optics for induced thermal treatment (hyperthermia) of tumors is one of the present-day tools to fight cancer [1–3]. Normal human tissues are highly scattering but weakly absorbing media in the wavelength range from about 0.6 to 1.4 μm providing a "therapeutic window". The absorption of laser light leading to a targeted heating of the tumor cells can be greatly increased by embedding silver or gold nanoparticles in the tumor. These nano-sized noble metal particles are characterized by strong resonance absorption and relatively weak scattering in the therapeutic window. Particularly, one can choose geometrical parameters of silica-core gold nanoshells to make these particles very good absorbers for the light of a widely used helium–neon laser of wavelength 0.6328 μm.

Thermal therapy of targeted cancer cells with the use of embedded gold nanoparticles is a promising new weapon in the battle against cancer, especially at the initial stage of the disease. A combination of hyperthermia with radiotherapy and chemotherapy has been shown to be effective in prolonging the survival of cancer patients. Many studies have been published on different aspects of the complicated and multi-faceted problem of thermal therapy. Theoretical studies have focused particularly on resonance optical properties of various gold nanoparticles in the visible and near infrared spectral ranges, modeling of propagation of laser radiation in human tissues with embedded nanoparticles, and developing of specific heat transfer models taking into account heat conduction, blood perfusion, metabolic heat generation, and radiative power absorbed in the processed tissues. A reader is directed to recent key publications [4–8] to learn about the state-of-the-art in this research field.

Prolonged direct heating of the tumor may lead to an unfavorable protective reaction of the thermal regulation system with an increase in blood perfusion near the tumor and release of heat shock proteins which are suggested to play a role in the process of thermotolerance [9]. Periodic heating with a single heating duration of about 10–15 s as suggested in [10] is a potential solution to decrease the blood flow variation but this remains to be proven.

A more radical change in the heating strategy proposed in the present paper is the use of indirect heating when the tumor is not subject to collimated laser radiation. One can consider two approaches in this indirect strategy:

1. The absorbing gold nanoparticles are embedded not in the tumor but in a circular region around the tumor. Laser heating of these particles leads to formation of a hot ring in the healthy tissue and the accumulated heat is conducted from all sides into

* Corresponding author. Tel.: +7 499 250 3264; fax: +7 495 362 5590.
E-mail address: ldombr@yandex.ru (L.A. Dombrovsky).

0017-9310/$ - see front matter © 2012 Elsevier Ltd. All rights reserved.
http://dx.doi.org/10.1016/j.ijheatmasstransfer.2012.04.029

Nomenclature

a	particle radius
A	Arrhenius' constant
c	specific heat capacity
C	coefficient introduced by Eq. (9)
D	radiation diffusion coefficient
E	function introduced by Eq. (9), activation energy
f_v	volume fraction of particles
F, G	functions introduced by Eq. (17)
h	heat transfer coefficient
I	radiation intensity
J	diffuse radiation intensity
k	thermal conductivity
L	thermal effect of chemical conversion
n	index of refraction
N	chemical reaction order
q	heat flux, radiative flux
Q	efficiency factor
r	radial coordinate
$\vec{r}$	spatial coordinate
R	reflectivity
t	time
T	temperature
u	velocity
v	perfusion rate
W	power
x	diffraction parameter
z	coordinate across the layer

Greek symbols

α	absorption coefficient
β	extinction coefficient
γ	coefficient introduced by Eq. (17)
δ	relative radius of the particle core
ε	volume fraction of blood
λ	wavelength
μ	cosine of an angle
$\bar{\mu}$	asymmetry factor of scattering
ξ	degree of thermal conversions
ρ	density
σ	scattering coefficient
τ	optical thickness
Φ	scattering phase function
ω	scattering albedo
$\vec{\Omega}$	unit vector of direction

Subscripts and superscripts

a	absorption, arterial blood
b	blood
c	cooling
ch	chemical
e	external
f	Fresnel's
h	heating
i	initial
m	metabolic
n	normal
r	radiative
s	scattering
t	tissue
tr	transport
v	venous blood
w	water
z	in z-direction
λ	spectral

the tumor. If the relative volume of the tumor is smaller than the volume of the hot ring, one can find a significant increase in the tumor temperature during the pause in periodic laser irradiation. Note that it may be difficult to supply gold nanoparticles in the circular region and control their distribution. This problem is of the rationale for the second approach or indirect strategy.

2. The laser irradiation of a circular region around the tumor is the same but there are no gold nanoparticles embedded in the tissue. In this case, the radiation is only partially absorbed in the circular volume of the body. The remaining part of this radiation is scattered in all directions and it is absorbed mainly in the tumor because of the higher absorption coefficient of the tumor tissue. This method is based on the relatively weak absorption of scattering human tissues in the therapeutic window.

When the heat front reaches the tumor boundary, the hypoxia effects are starting to play important role. A combination of the above approaches using a low volume fraction of gold nanoparticles may be a reasonable choice. In particular, one can place gold nanoparticles at the tumor periphery to increase the local absorption of laser radiation scattered by a surrounding healthy tissue. Note that relative contribution of scattered radiation to the radiative heating of the tumor may be insignificant in two limiting cases: at very low and very high scattering of ambient tissues. So, one should examine if this effect is really important for the particular problem under consideration.

It is important that the use of the above described indirect strategy may be and should be combined with water cooling of the irradiated body surface where highly sensitive pain receptors are very close to the body surface. This surface cooling is expected to decrease significantly the pain accompanied strong heating of a very thin surface layer in the case of the direct laser treatment. This more comfortable indirect heating may permit a more prolonged treatment of the tumor leading to a better soft hyperthermia regime.

Obviously, the simplified one-dimensional models of laser-induced hyperthermia [10,11] are not appropriate for the computational analysis of the indirect heating strategy. Therefore, the main objective of the present paper is to develop a more sophisticated two-dimensional model taking into account the realistic shape of a superficial tumor, blood perfusion through capillaries, the volumetric heat transfer between arterial blood and tissue, and also thermal conversions in venous blood and tumor tissue during hyperthermia. Another objective of the present study is to analyze numerically the advantages and possible drawbacks of the indirect heating strategy with or without embedded gold nanoshells. As this is a very complex problem, it is important to investigate the relative contribution of different physical processes and their parameters to the resulting characteristics of thermal degeneration of tumor cells. This experience can be used to simplify the computational model and avoid detailed modeling of the processes which appear not to be of great importance.

In contrast to [10,11], we analyze not only the absorbed radiation power and temperature field but consider also a degree of thermal conversions in both venous blood and ambient tissue. This makes the computational results much closer to medical practice because the desirable effect cannot be described correctly in the terms of either the maximum temperature or the absorbed energy.

The latter statement seems to be obvious. Nevertheless, most of authors of medical papers are convinced that the single important factor is the treatment temperature whereas there are strong opposing opinions, which declare that the delivered heat (absorbed energy) is of primary importance. These two approaches are discussed in some detail by Szasz et al. [12] (see also [13]), where one can also find useful references.

It is known that few measurable effects are observed below 42 °C and the first mechanism by which biological tissue is thermally affected can be attributed to some molecular changes [14]. These effects, accompanied by bond destruction and membrane alterations, are summarized in the term hyperthermia in the range from about 42 to 50 °C. If such a hyperthermia lasts for several minutes, a significant percentage of the cancerous tissue will undergo necrosis [14]. The thermal problem of hyperthermia is considered by taking into account the kinetics of the cell destruction processes as described by the Arrhenius-type equations. Of course, the Arrhenius equation parameters for blood and tissue are different. Moreover, one should use different parameters in different temperature ranges for every substance or include several terms in the kinetic equation to take into account a set of various degradation processes.

Complete calculations for a model problem with realistic parameters of human tissues are given in the paper. It should be emphasized that the model developed cannot include all processes which may be important at some specific conditions. We avoid also overloading of the model by accounting for some insignificant details. Nevertheless, we believe that the presented example problem is much closer to the current medical practice than a simplified one-dimensional problem considered in our recent paper [10].

2. Radiative transfer modeling

In our study, we employed a continuum approach to model the radiative transfer in a complex medium containing scattering (and weakly absorbing) tissue and absorbing (and weakly scattering) nanoparticles. The so-called radiative transfer equation (RTE) is considered in the traditional continuum theory. In the case of a negligible emission of the radiation by a scattering and absorbing medium, the RTE for randomly polarized radiation can be written as follows [15–17]:

$$\vec{\Omega}\nabla I_\lambda(\vec{r},\vec{\Omega}) + \beta_\lambda I_\lambda(\vec{r},\vec{\Omega}) = \frac{\sigma_\lambda}{4\pi}\int_{(4\pi)} I_\lambda(\vec{r},\vec{\Omega}')\Phi_\lambda(\vec{\Omega}'\vec{\Omega})d\vec{\Omega}' \quad (1)$$

The physical meaning of Eq. (1) is evident: variation of the spectral radiation intensity in direction $\vec{\Omega}$ takes place due to extinction by absorption and by scattering in other directions, as well as due to scattering from other directions (the integral term). The absorption coefficient, α_λ, the scattering coefficient, σ_λ, and scattering phase function, Φ_λ, depend on the coordinate $\vec{r}$. For simplicity, Eq. (1) is written for the case of an isotropic medium when the coefficients of RTE do not depend on direction. One can also consider a general case of anisotropic medium but this is not so important for optically thick highly scattering tissues [15,18].

A complete and accurate solution to the RTE in scattering media is a very complicated task because of the integral term in the right-hand side of the RTE. One can find many studies in the literature on specific numerical methods developed to obtain more and more accurate spatial and angular characteristics of the radiation intensity field. Several modifications of the discrete ordinates method (DOM) and statistical Monte Carlo (MC) methods are the most common tools employed by many authors [15–17]. As to the applied problem under consideration, one can refer to recent papers by Fasano et al. [19] and Banerjee and Sharma [20] where the MC method is used in biomedical applications.

To avoid additional mathematical complexity, we prefer to use a simplified approach to the problem and focus on analysis of the interaction of physical processes. The specific problem statement makes possible the use of the well-known transport approximation for the scattering phase function [15]. According to this approximation, the scattering phase function is replaced by a sum of the isotropic component and the term describing the peak of forward scattering:

$$\Phi_\lambda(\mu_s) = (1-\bar{\mu}_\lambda) + 2\bar{\mu}_\lambda\delta(1-\mu_s) \quad (2)$$

With the use of transport approximation, the RTE can be written in the same way as that for isotropic scattering, i.e. with $\Phi_\lambda \equiv 1$:

$$\vec{\Omega}\nabla I(\vec{r},\vec{\Omega}) + \beta_{tr} I(\vec{r},\vec{\Omega}) = \frac{\sigma_{tr}}{4\pi}\int_{(4\pi)} I(\vec{r},\vec{\Omega})d\vec{\Omega} \quad (3)$$

Hereafter, the subscript λ is omitted for brevity. The transport approximation has been widely used in radiative transfer calculations for many years. It has been confirmed that hemispherical characteristics of a radiation field in highly scattering materials are well described using this approximation [15,21]. The latter makes the quantity σ_{tr} to be the most important scattering property of the medium.

An axisymmetric problem for laser induced hyperthermia of a superficial tumor is considered in the present paper. The problem statement is based on the following assumptions:

- The axis of the computational region coincides with the normal to a flat surface of a healthy body (without tumor). The laser beam is directed along the axis of the computational region.
- The body surface is optically smooth. This allows the use of Fresnel's relations for reflection and refraction of the direct and scattered laser radiation at the body surface. This assumption may seem to be not realistic but this is compensated by a significant volumetric scattering of the radiation by human tissues.
- The gold nanoshells are embedded in a finite circular volume around the tumor. This volume (particle cloud) is a small part of the computational region. The volume fraction of gold nanoshells can be an arbitrary function of radial and axial coordinates but it is independent of time (this assumption can be revised later).
- The tissue index of refraction is uniform in the computational region. Strictly speaking, there is a spatial variation of the refractive index in the real multi-layer tissue. This variation can be taken into account in a modified version of the computational model. Note that correct description of the radiation propagation in a medium with variable refractive index is a significantly more complicated task even in the case of a one-dimensional problem [22].

A solution for the directional component of the radiation intensity appears to be not as simple as that for 1-D problem [10] because of a relatively complex path of refracted and reflected beam. To simplify the mathematics, we used an additional assumption of a small angle between the current normal to the body surface and the normal to the flat healthy body surface. The resulting simplification is obvious: we can use the local 1-D solution for the directional radiation component. As to the diffuse radiation component, it can be determined using the well-known P_1 approximation. Note that the expected error of the P_1 increases significantly in 2-D problems with nonuniform spatial distribution of the medium properties and the radiation power [15].

The schematic of the particular example problem for a skin cancer is presented in Fig. 1. A circular laser beam with a uniform distribution of the incident radiation power for $5 < r < 10$ mm is

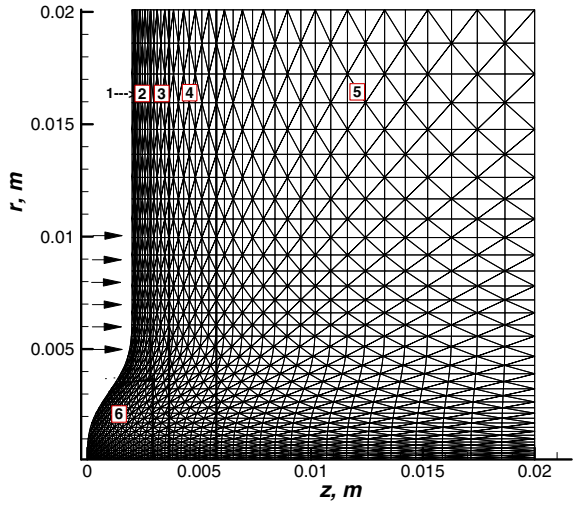

Fig. 1. Schematic of an axisymmetric computational region and FEM triangulation; 1, 2,. . ., 6 – the numbers of various tissues listed in Table 1.

considered. The radiative properties of tissues in the superficial layers are specified in Table 1. Following Vera and Bayazitoglu [11] the laser with wavelength of $\lambda = 0.6328$ μm was used so the absorption coefficient and transport scattering coefficient of tissues at this wavelength were taken from the literature [23–26]. Note that absorption and scattering coefficients of a composite medium which can be treated as a matrix (host medium) containing a not too high volume fraction, f_v, of small spherical particles of the same radius a can be calculated using the following simple relations [15]:

$$\alpha = \alpha_t + 0.75 f_v \frac{Q_a}{a}, \quad \sigma_{tr} = \sigma_{tr,t} + 0.75 f_v \frac{Q_s^{tr}}{a} \tag{4}$$

where Q_a and Q_s^{tr} are the dimensionless efficiency factor of absorption and transport efficiency factor of scattering for single particles. The first terms in relations (4) correspond to the host medium whereas the second terms are the contributions due to embedded particles. Following paper [10], we consider the following parameters of gold-coated silica nanoshells:

$$a = 20\ \text{nm}, \quad \delta = 0.725, \quad Q_a = 7.828, \quad Q_s^{tr} = 1.144 \tag{5}$$

The above values of efficiency factors were calculated using the Mie theory [27] at tissue index of refraction $n_t = 1.45$. For simplicity, it is assumed that volume fraction of gold nanoshells is uniform in the "particle cloud". In an example problem considered in this paper, the particle cloud is positioned between radii 5 and 10 mm (just opposite the laser beam) from the body surface to the plane $z = 4$ mm (see Fig. 1). Note that irradiated area of the body surface is equal to 236 mm^2. It should be noted that an annular region of irradiation can be formed by scanning the annulus with a relatively narrow laser beam.

The shadow boundaries of the computational region are characterized by a surface albedo. In other words, we should take into account the radiation scattered from the medium beyond the computational region. The boundary conditions for Eq. (3) are:

$$\text{At the body surface}: I(\vec{r}, \vec{\Omega}\vec{n}) = R_f(\vec{\Omega}\vec{n}) I(\vec{r}, -\vec{\Omega}\vec{n}) + (1 - R_f) q_e \delta(1-\mu) \quad \vec{\Omega}\vec{n} > 0 \tag{6a}$$

$$\text{At other surfaces}: I(\vec{r}, -\vec{\Omega}\vec{n}) = R_t(\vec{\Omega}\vec{n}) I(\vec{r}, \vec{\Omega}\vec{n}) \quad \vec{\Omega}\vec{n} > 0 \tag{6b}$$

where q_e is the incident radiative flux, $R_f(\mu)$ is the Fresnel's reflectivity [28]:

$$R_f = (R_\parallel + R_\perp)/2 \tag{7a}$$

$$R_\parallel = \left\{ \frac{\mu - n_t \sqrt{1 - n_t^2(1-\mu^2)}}{\mu + n_t \sqrt{1 - n_t^2(1-\mu^2)}} \right\}^2, \quad R_\perp = \left\{ \frac{n_t \mu - \sqrt{1 - n_t^2(1-\mu^2)}}{n_t \mu + \sqrt{1 - n_t^2(1-\mu^2)}} \right\}^2 \quad \text{when} \quad \mu > \mu_{cr} \tag{7b}$$

$$R_\parallel = R_\perp = 1 \quad \text{when} \quad \mu \le \mu_{cr} = \sqrt{1 - 1/n_t^2} \tag{7c}$$

We assume here that the tissue index of absorption is relatively small: $\kappa_t << n_t$. The value of $R_f = 1$ for $\mu \leqslant \mu_{cr}$ corresponds to the total internal reflection. The reflectivity R_t for the scattering tissue at the other boundaries of the computational region will be determined below.

Following the usual technique, present the radiation intensity I as a sum of the diffuse component J and the term, which corresponds to the transmitted and reflected directional external radiation:

$$I = J + \frac{1 - R_{f,n}}{1 - R_{f,n} C_{tr}} [E\delta(1-\mu) + (C_{tr}/E)\delta(1+\mu)] q_e \tag{8}$$

where $R_{f,n} = R_f(1)$ and $R_{t,n} = R_t(1)$ are the normal reflectivities and

$$E = \exp(-\tau_{tr}) \quad \tau_{tr} = \int_0^z \beta_{tr} dz, \quad C_{tr} = R_{t,n} \exp(-2\tau_{tr}^0), \quad \tau_{tr}^0 = \int_0^d \beta_{tr} dz \tag{9}$$

The mathematical problem statement for the diffuse component of radiation intensity is as follows:

$$\vec{\Omega}\nabla J + \beta_{tr} J = \frac{\sigma_{tr}}{4\pi}(G + F), \quad G = \int_{(4\pi)} J d\vec{\Omega}, \quad F = \frac{1 - R_{f,n}}{1 - R_{f,n} C_{tr}} (E + C_{tr}/E) q_e \tag{10}$$

$$\text{At the body surface}: J(\vec{r}, \vec{\Omega}\vec{n}) = R_f(\vec{\Omega}\vec{n}) J(\vec{r}, -\vec{\Omega}\vec{n}), \quad \vec{\Omega}\vec{n} > 0 \tag{11a}$$

$$\text{At other surfaces}: J(\vec{r}, \vec{\Omega}\vec{n}) = R_t(\vec{\Omega}\vec{n}) J(\vec{r}, -\vec{\Omega}\vec{n}), \quad \vec{\Omega}\vec{n} > 0 \tag{11b}$$

The spectral radiation power absorbed in the medium, W, is expressed as

$$W = -\nabla \vec{q} = -\int_{(4\pi)} \vec{\Omega}\nabla I d\vec{\Omega} = \alpha(G + F) \tag{12}$$

As it was done in [10], we use the following equations for normal reflectivities:

$$R_{f,n} = \left(\frac{n_t - 1}{n_t + 1} \right)^2 \quad R_{t,n} = \frac{\omega_{tr}^e}{(1 + \sqrt{1 - \omega_{tr}^e})(1 + 2\sqrt{1 - \omega_{tr}^e})} \tag{13}$$

where $\omega_{tr}^e = \sigma_{tr}^e / \beta_{tr}^e$ is the transport albedo of a healthy tissue outside the computational region.

The above formulated problem for the diffuse component of the radiation intensity is still very complex. Therefore, the first-order

Table 1
Radiative properties of tissues in the computational region.

Tissue number	1	2	3	4	5	6
Tissue name	Epidermis	Papillary dermis	Reticular dermis	Fat	Muscle	Tumor
α, 1/mm	0.3	0.27	0.27	0.19	0.12	2.0
σ_{tr}, 1/mm	2.5	3.75	3.75	2.7	0.9	7.5

approximation of the spherical harmonics method (P_1) [15] is considered as a regular method to solve this problem. In this approximation, the following linear presentation for the angular dependence of radiation intensity is considered:

$$J(\vec{r},\vec{\Omega}) = \frac{1}{4\pi}[G(\vec{r}) + 3\vec{\Omega}\vec{q}(\vec{r})] \tag{14}$$

Obviously, this model angular dependence of the diffuse radiation intensity is not correct near the boundaries of the computational region. Nevertheless, it is known that P_1 gives usually rather good results for the radiation flux divergence (the absorbed radiation power), which is important for our problem. The latter statement is true for the region part with a relatively high radiation power density, but the error increases towards sub-regions with not so high volumetric radiation power. Note that P_1 approximation has been characterized in recent review paper by Feng and Fuentes [29] as a good approach for modeling laser-induced thermal therapy. One should recall here a general computer code LATIS for laser-tissue interaction modeling [30]. The Monte Carlo method is mainly used in this code, but there is an ability to invoke P_1 approximation to avoid very time-consuming calculations. Note that the general discrete ordinates method is also used in some papers to calculate accurately radiative transfer in human tissues [31].

After some transformations, the following simple boundary value problem of P_1 approximation can be obtained:

$$-\nabla(D\nabla G) + \alpha G = \sigma_{tr} F \tag{15}$$

$$\text{At the body surface}: \quad -D(\vec{n}\nabla G) = \frac{\gamma_f}{2} G \tag{16a}$$

$$\text{At other surfaces}: \quad -D(\vec{n}\nabla G) = \frac{\gamma_t}{2} G \tag{16b}$$

where

$$D = \frac{1}{3\beta_{tr}}, \quad \gamma_f = \frac{1 - R_{f,n}}{1 + R_{f,n}}, \quad \gamma_t = \frac{1 - R_{t,n}}{1 + R_{t,n}} \tag{17}$$

Note that the Marshak boundary conditions were used in the above formulation.

It is not difficult to proceed to the variational formulation of the problem (15) – (16) when the solution yields the minimum of the following functional:

$$\chi = \int_V \left[\frac{D}{2}(\nabla G)^2 + \frac{\alpha}{2}G^2 - \sigma_{tr} F G\right] dV + \int_S \frac{\gamma}{2} G^2 dS \tag{18}$$

The order of the differential operator in (18) is reduced by one compared with (15). As a result, the transition to the variational formulation is convenient for the use of finite-element method (FEM) with not high local approximation order of the function to be found. With the unified program blocks of FEM, the arrangement of computer codes for the calculation of the multi-dimensional radiation field is considerably simplified. The extensive possibilities of FEM in the description of complex form regions with nonuniform properties of the medium provide the universality of the algorithm. In accordance with the general FEM scheme, we will divide a computational region into sub-regions, or finite elements, and suppose that the unknown function can be presented as a polynomial in every element. For the sake of simplicity, only triangular elements are considered (see Fig. 1) with linear approximation of the function G in the element.

The computational region is rather large because we are going to calculate transient heat transfer during a prolonged periodic laser heating. As to the particular radiative transfer problem, it would be sufficient to consider a part of the computational region. This is explained by the rather high scattering of laser radiation in human skin. Nevertheless, it was convenient to conduct all the calculations using the same complete finite-element mesh.

The numerical results for the absorbed radiation power are presented in Fig. 2. One can see that the part of the laser radiation power absorbed in a thin surface layer of the body is greater when gold nanoshells are imbedded in the tissue. At the same time, the two fields of the absorbed radiation power (with or without gold nanoshells) are similar to each other. It means that the effect of scattering towards the tumor appears to be insignificant even in the case when there are no gold nanoshells in the body. This result is explained by a very high transport scattering coefficient when the multiple scattering of radiation in a thin surface layer leads to the absorption of the radiation in the tissue even at low spectral absorption coefficient. It follows that in this case an error of P_1 approximation is negligibly small, and there is no need to verify this approach in this particular situation, which is very close to the 1-D radiative transfer problem. Note that the use of a nonuniform computational grid with 3200 triangular elements appeared to be sufficient even for radiative part of the problem

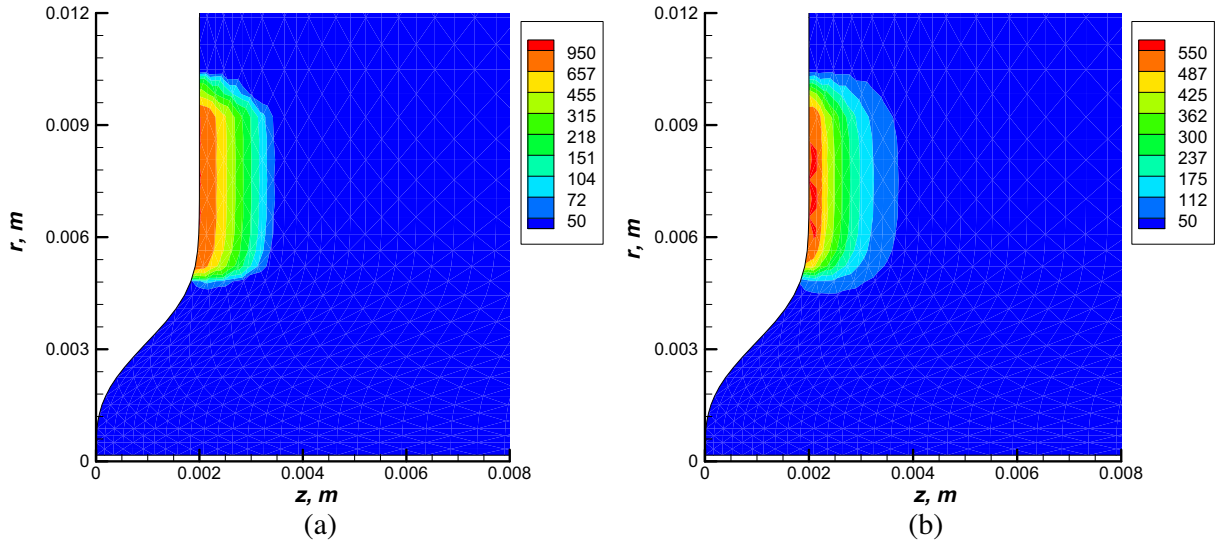

Fig. 2. Absorbed volumetric radiation power: a – with gold nanoshells, b – without gold nanoshells. The value per unit incident radiation flux (in m^{-1}) is plotted.

under consideration. It was confirmed by direct calculations with the double number of grid intervals in every direction, i.e. by the use of a similar grid with 12800 finite elements.

3. Transient heat transfer model

The energy transport in a biological system is usually expressed by the so-called bioheat equation. The bioheat equation developed by Pennes [32] is one of the earliest models for energy transport in tissues. Pennes assumed that the arterial blood temperature, T_b, is uniform throughout the tissue while the venous blood temperature is equal to the local tissue temperature T_t. The resulting transient energy equation is as follows:

$$\rho c\frac{\partial T_t}{\partial t} = \nabla(k\nabla T_t) + \rho_b c_b v_b(T_b - T_t) + W_m \tag{19}$$

where the second term on the right-hand side is responsible for the heat transfer due to arterial blood perfusion of rate v_b, and the last term W_m is the metabolic heat generation within the tissue. A more detailed model for heat transfer in human tissues should be based on two coupled energy equations for the tissue and artery blood with the spatial and time variation of arterial blood temperature is taken into account in such a model [4,6]. In the present paper, the following coupled energy equations similar to those described in [4,6] are considered:

$$(1-\varepsilon_a)(\rho c)_t\frac{\partial T_t}{\partial t} = \nabla[(1-\varepsilon_a)k_t\nabla T_t] + h_{b,t}(T_b - T_t) + (1-\varepsilon_a)W_m + \left(1-\varepsilon_a\frac{\alpha_b}{\alpha}\right)W + W_{ch} \tag{20a}$$

$$\varepsilon_a(\rho c)_b\left(\frac{\partial T_b}{\partial t} + \vec{u}_b\nabla T_b\right) = \nabla[\varepsilon_a k_b\nabla T_b] - h_{b,t}(T_b - T_t) + \varepsilon_a\frac{\alpha_b}{\alpha}W \tag{20b}$$

where ε_a is the volume fraction of arterial blood, α_b is the spectral absorption coefficient of arterial blood. The volumetric heat generation due to absorption of laser radiation is taken into account in both energy equations. Of course, this heat is not uniformly absorbed in a composite medium characterized by the total absorption coefficient α. Therefore, the corresponding terms in Eqs. (20a) and (20b) are different. It is important that the ratio α_b/α is greater in the case when there are no highly absorbing gold nanoshells in ambient tissue. In this case, the radiative heat generation in arterial blood may be considerably greater than that in the tissue. This effect is known, and it is used in selective thermal heating and damage of blood by action of a pulsed laser radiation at wavelength $\lambda = 0.532$ μm or 0.585 μm characterized by extremely high spectral values of α_b [33,34]. It is clear that the same effect of relatively strong absorption of laser radiation takes place also for venous blood. The latter may be a physical basis for more detailed three-temperature heat transfer model with a third energy equation for venous blood. This general model is not considered in the present paper because we consider the wavelength $\lambda = 0.6328$ μm characterized by minimum value of α_b and more appropriate for the soft thermal treatment.

The term W_{ch} in Eq. (20a) takes into account the heat of endothermic chemical conversions in human tissues and venous blood during a strong hyperthermia. In the latter case, one can use the following relation for this term:

$$W_{ch} = (1-\varepsilon_a-\varepsilon_v)L_t\frac{\partial\rho_t}{\partial t} + \varepsilon_v L_v\frac{\partial\rho_v}{\partial t} \tag{21}$$

where ε_v is a volume fraction of venous blood ($\varepsilon_v + \varepsilon_a = \varepsilon$), and L_t, L_v are the specific thermal effects of chemical conversions in tissue and venous blood. Strictly speaking, one can also consider the thermal effect of filtration of some gaseous products of these chemical conversions as it is usually considered in engineering problems for thermal destruction of organic composite materials [35,36]. But we will not do it in our model for the soft thermal treatment. Moreover, we will neglect the chemical term W_{ch} because the values L_t and L_v are not known and the heating process is rather slow. The latter enables us to assume that a contribution of endothermic chemical conversions to the heat balance is relatively small. It does not mean that we should not calculate time variation of the local degree of chemical conversions because this value is one of the main parameters of the thermal treatment.

The energy equations (20a,b) for arterial blood and other tissues are based on a presentation of the real complex tissue as a two-temperature continuous porous medium. It is assumed that there are no big blood vessels in the computational region. As to arterial blood velocity, it can be determined using additional Darcy-type equation for filtration of the blood. In this paper, we do not consider any variation of the arterial blood flow. Instead, the field of this physical quantity, $\vec{u}(\vec{r})$, is assumed to be known. The fields of $\varepsilon_a(\vec{r})$ (the volume fraction of arterial blood) and $h_{b,t}(\vec{r})$ (the volumetric heat transfer coefficient between arterial blood and ambient tissue) are also considered as input parameters of the problem. These parameters depend on the fine structure of the peripheral vascular system.

Neglecting the chemical conversion terms in Eq. (20a) and also the variation of thermal and optical properties of a composite medium with the degree of these conversions simplifies significantly the problem statement. It appears to be sufficient to calculate the chemical conversion parameters at every time moment after the temperature field calculations. This can be done using the following kinetic equations for thermal conversion of venous blood and tissues:

$$\frac{\partial\xi_b}{\partial t} = (1-\xi_b)^{N_b}A_b\exp\left(-\frac{E_b}{RT_t}\right) \tag{22a}$$

$$\frac{\partial\xi_t}{\partial t} = (1-\xi_t)^{N_t}A_t\exp\left(-\frac{E_t}{RT_t}\right) \tag{22b}$$

Following [37] we assume that the orders of chemical reactions in Eq. (22) are equal to unity: $N_b = N_t = 1$. Introduced in 1947 [38,39], the idea to quantify thermal damage, specifically for tissue, was originally based on a first-order chemical reaction rate proposed by Svante Arrhenius to characterize pathological transformation from one state to another. However, available experimental data suggest that there may be two transitional temperatures around 43 °C and 52 °C in the temperature range from 39 to 60 °C [29]. To overcome the weakness of the one-stage Arrhenius model described above, other types of models have been proposed for thermal damage of cells and tissues. One can find more details on this subject in review paper by Feng and Fuentes [29]. The parameters of advanced kinetic models for various tissues are not well known at the moment. Therefore, the simplest kinetic relations (22) are used in the present study.

It should be noted that thermal conductivity and especially the radiative properties of a tissue containing damaged cells are expected to be different from those of healthy tissue and there are some data in the literature on this subject [33,37,40]. Particularly, the spectral absorption coefficient and transport scattering coefficient of a damaged tissue is usually much greater than the corresponding properties of a healthy tissue [33,41,42]. It means that a complete heat transfer model should include repeating calculations of the radiation field at every time step of the numerical solution for the transient problem. These nonlinear effects may lead to considerable correction of the final results. Nevertheless, this analysis is not presented here because of the limited length of the journal paper. The authors are planning to undertake a computational study of the above nonlinear effects in the nearest future.

The initial and boundary conditions for Eq. (20a) are as follows:

$$t = 0, \quad T_t = T_{t,i}(z,r) \tag{23}$$

$$z = 0, \quad 0 < r < R_1 \quad \text{or} \quad R_2 < r < R, \quad k\frac{\partial T_t}{\partial z} = h_1(T_{e,1} - T_t) \tag{24a}$$

$$z = 0, \quad R_1 < r < R_2, \quad k\frac{\partial T_t}{\partial z} = h_w(T_w - T_t) \tag{24b}$$

$$r = 0, \quad \frac{\partial T_t}{\partial r} = 0 \qquad r = R, \quad \frac{\partial T_t}{\partial r} = 0 \tag{24c}$$

$$z = H, \quad k\frac{\partial T_t}{\partial z} = h_2(T_{e,2} - T_t) \tag{24d}$$

The boundary condition (24a) is the natural convective heat transfer with ambient air, the condition (24b) refers to the water cooling of the body surface (using a transparent water jacket), the conditions (24c) are the symmetry and adiabatic conditions, the condition (24d) describes approximately the heat transfer from the internal part of the body, which has a constant temperature $T_{e,2}$. The initial steady-state temperature profile $T_i(z,r)$ in Eq. (23) is a solution to the following boundary-value problem:

$$\nabla[(1-\varepsilon)k_t\nabla T_{t,i}] + h_{b,t}(T_b - T_{t,i}) + (1-\varepsilon)W_m = 0 \tag{25}$$

$$z = 0, \quad k\frac{dT_{t,i}}{dz} = h_1(T_e - T_{t,i}) \tag{26a}$$

$$r = 0, \quad \frac{\partial T_{t,i}}{\partial r} = 0 \qquad r = R, \quad \frac{\partial T_{t,i}}{\partial r} = 0 \tag{26b}$$

$$z = H, \quad k\frac{\partial T_{t,i}}{\partial z} = h_2(T_{e,2} - T_{t,i}) \tag{26c}$$

Of course, there is no water cooling before the thermal treatment.

As to the boundary conditions for Eq. (20b) (for arterial blood), these are slightly different at the body surface and at the boundary with the rest massive body:

$$T_b = T_t \quad \text{at the body surface} \tag{27a}$$

$$T_b = T_b^e \quad \text{at} \quad z = H \tag{27b}$$

In our calculations, we assume that $T_b^e = T_{e,2}$.

It should be noted that a realistic picture of the arterial blood flow cannot be described adequately on the basis of the 2-D axisymmetric problem. To clarify this statement, consider the main features of the vascular system in a typical superficial layer of a human body. One should distinguish five different zones of this system:

- There are no blood vessels in the epidermis layer;
- The layers of dermis are characterized by a dense network of fine blood vessels (capillaries). Both the axial and average radial components of the blood velocity are equal to zero in this layer.
- The fat layer contains some blood vessels oriented approximately along the axis of our computational region. The arterial blood flows towards the body surface in this layer and the axial component of the blood velocity can be taken into account in the above suggested model.
- The muscle layer contains comparatively large vessels. An average flow rate of arterial blood in this layer is much greater than that in the dermis layers. The network of blood vessels can be usually characterized by a definite direction along the body surface. As for average radial velocity of arterial blood (in terms of our computational model) it is equal to zero, as well as the axial component of the blood velocity.
- The tumor region has an extremely dense network of randomly oriented blood capillaries which averaged over all orientations gives a zero velocity of arterial blood.

Therefore, the only nonzero contribution of the blood flow to the convective term of Eq. (20b) is present in the fat layer. However, as the volume fraction of arterial blood is very small in this layer, we will neglect the convective term in the example problem considered below. At the same time, the volumetric heat transfer between the arterial blood and ambient tissues in the dermis, fat and muscle layers, and especially in the tumor cannot be ignored. It is natural to assume that the value of $h_{b,t}$ is directly proportional to the volume fraction of arterial blood in each of the above zones.

4. Results of heat transfer calculations

In the example problem, the conditions of the experimental study by Çetingül and Herman [43,44] were used to determine a steady-state temperature profile in the tissue without laser treatment. According to the measurements of [43] the ambient temperature and heat transfer coefficient were taken equal to T_e = 22.5 °C and h_1 = 10 W/(m^2 K). To calculate the heat flux from the body to the surface layer, we used value of $T_{e,2}$ = 37 °C and estimated value of h_2 = 50 W/(m^2 K). Water cooling during radiation was imposed at the irradiated surface between R_1 = 5 mm and R_2 = 10 mm with

Table 3
Thermal properties and spectral absorption coefficient of blood.

ρ_t, kg/m^3	c_t, J/(kg K)	α_b, 1/mm (at λ = 0.633 μm)
1060	3600	0.21

Table 4
Pre-exponential factor (Arrhenius' constant) and activation energy for cell destruction.

	A, 1/s	E, kJ/mol
Tissue	3.1 10^{98}	628
Blood	7.6 10^{66}	448

Table 2
Thermal properties of tissues in the computational region.

Layer number	1	2	3	4	5	6
Tissue name	Epidermis	Papillary dermis	Reticular dermis	Fat	Muscle	Tumor
ρ_t, kg/m^3	1200	1200	1200	1000	1085	1030
c_t, J/(kg K)	3589	3300	3300	2674	3800	3582
k_t, W/(m K)	0.235	0.445	0.445	0.185	0.51	0.558
W_m, W/m^3	0	368.1	368.1	368.3	684.2	9000
ε_a, %	0	0.15	0.96	0.07	2.0	6.5
ω_a, 10^{-3} s^{-1}	0	0.2	1.3	0.1	2.7	6.3
$h_{b,t}$, kW/(m^3 K)	N/A	0.79	5.15	0.27	11.13	23.24

T_w = 35 °C and h_w = 10^3 W/(m^2 K). For the case with embedded gold nanoshells, we used the volume fraction $f_v = 10^{-6}$.

The optical properties of the human tissues are specified in Table 1 and thermal properties – in Table 2. The data for the absorption and transport scattering coefficients were taken from [23,45]. The data for the tissue density, specific heat capacity, thermal conductivity, and metabolic heat generation power in healthy tissues as well as dimensions of the skin sub layers were taken from [43,44]. The metabolic heat generation in the tumor is not so definite a parameter because it is almost inversely proportional to the characteristic time of the tumor growth [46]. The value of W_m in Table 2 was chosen to obtain a small overheating of the tumor region before the treatment.

In the example problem, we ignore the possible effect of increase in thermal conductivity of human tissues due to the presence of gold nanoshells. Obvious estimates confirm that this assumption is acceptable in the case when there is no abnormal change in thermal conductivity reported in some recent papers on nanofluids [47–52]. The latter problem is beyond the scope of the present study.

A variation of the local blood perfusion with temperature studied in [53–56] was neglected in the present calculations. This effect may be important in the case of a long-time thermal treatment and could be studied at the next stage of the computational analysis of the problem.

To calculate the coefficients of the radiation terms in energy Eq. (20) one should know the spectral absorption coefficient of human blood. This value was taken from [57]. Thermal and optical properties of blood used in the calculations are presented in Table 3. It should be emphasized that absorption coefficient of blood depends strongly on the radiation wavelength and may be much greater than comparatively small value of α_b used in the present paper (see [57–60]). High values of α_b may lead to strong local overheating of blood with respect to tissue. This effect is not desirable in soft hyperthermia but it is widely used for the targeted thermal treatment of blood in the case of some specific deceases [34,61].

According to [14,33] we use the Arrhenius law parameters (pre-exponential factor and activation energy) specified in Table 4. These parameters are used to estimate possible partial destruction of both tissue and blood. According to [62] there are some important conversions in tumor tissue at lower temperatures (about 40–42 °C) when the cells are not destroyed but arterial blood cannot supply sufficient oxygen to the tumor and some bonds in tumor molecules are damaged. These processes can be also approximately described in terms of Arrhenius-type kinetic equations [62].

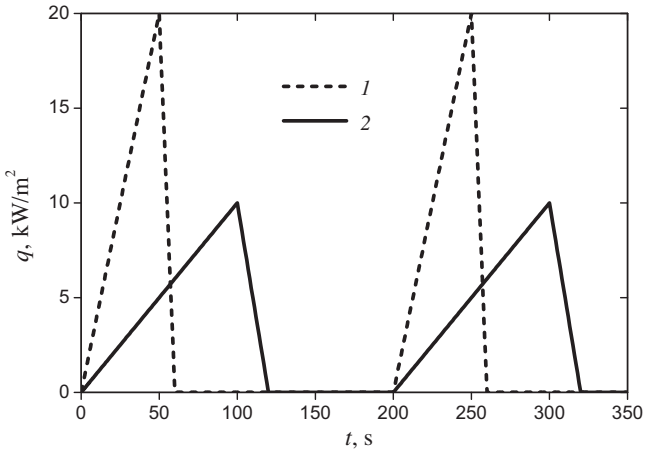

Fig. 4. Fragments of time dependences of the incident radiative flux in periodic heating: 1 and 2 – numbers of the heating regimes.

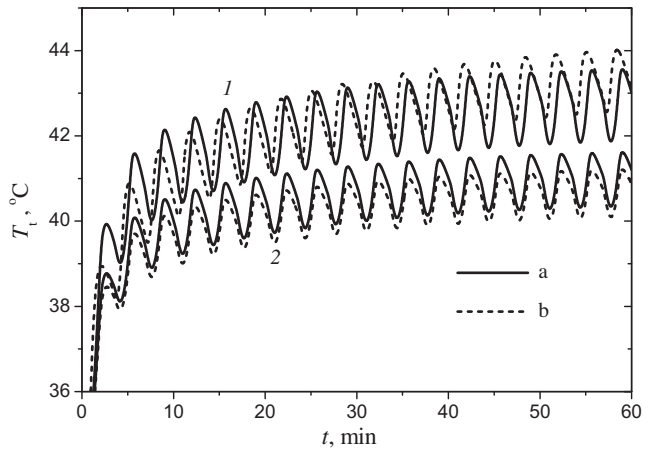

Fig. 5. Time variation of tissue temperature in the tumor center: a – with embedded gold nanoshells, b – without gold nanoshells; 1 and 2 – numbers of the heating regimes presented in Fig. 4.

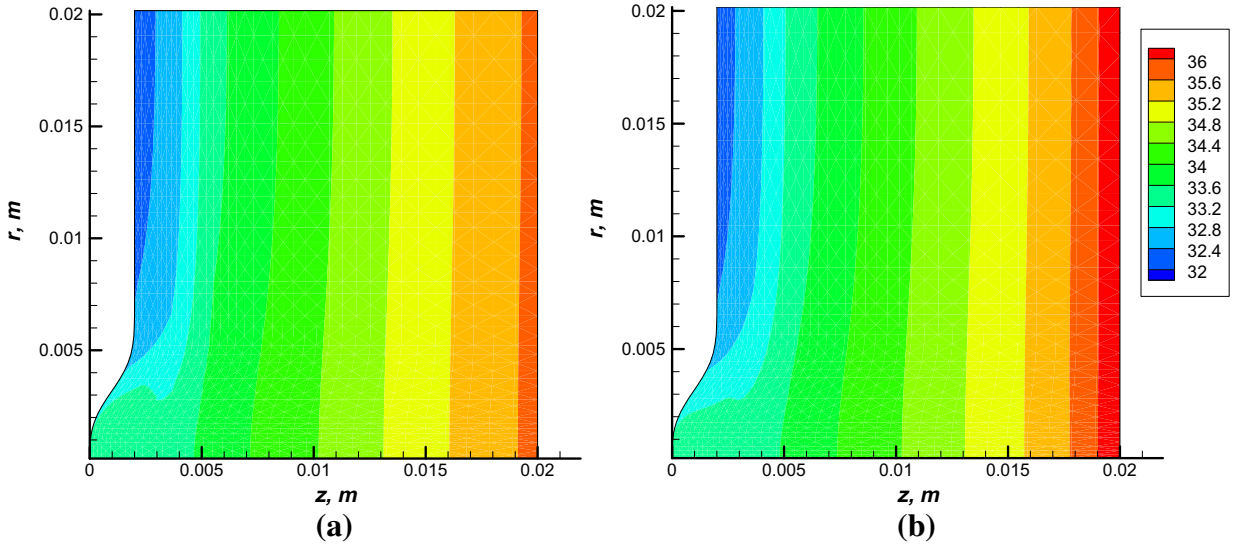

Fig. 3. Steady-state temperature field in non-irradiated body (before the thermal treatment): a – human tissue, b – arterial blood.

Fig. 3 shows the computational results for a steady thermal state of the superficial layers of the body. It can be seen that there is a considerable rise of the tumor temperature due to metabolic heat generation and that the arterial blood temperature is slightly less that the temperature of the tissue in this region. This temperature fields were used as the initial conditions for subsequent transient heat transfer calculations of the laser-induced hyperthermia process.

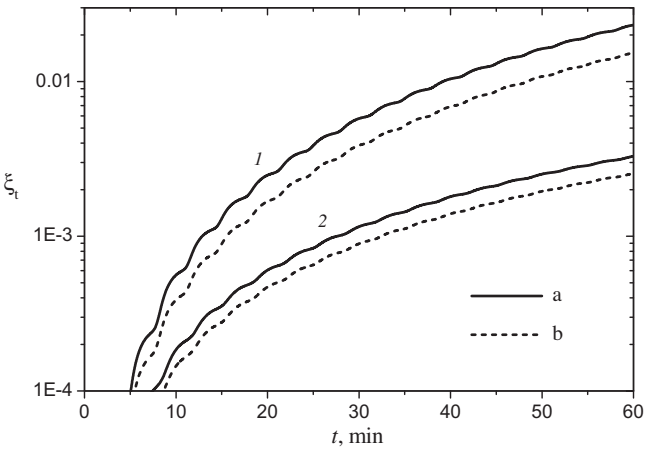

Fig. 6. Degree of thermal destruction of tissue cells in the tumor center. The designations see in Fig. 5.

Two possible regimes of a periodic laser heating have been considered (see Fig. 4). A perfect external thermal insulation of the tumor surface was assumed to obtain more uniform temperature field in the tumor. Two periodic time dependences of the incident radiative flux were chosen to reach the desirable tumor temperature without strong overheating of the directly irradiated tissue. These two regimes are characterized by slow time variations of the incident radiative flux and the same total energy per one period of irradiation. This energy is equal to 0.142 J.

The results for time variation of the tissue temperature in a point which is close to the center of the tumor (at a distance about 1 mm from the external tumor surface) for periodic regimes of irradiation are presented in Fig. 5. It can be seen that this temperature is characterized by oscillations with a period of 200 s which is the same for both regimes of laser irradiation shown in Fig 4. The calculated tumor temperature is shown to be weakly sensitive to the presence of gold nanoshells. It means that there is no need to

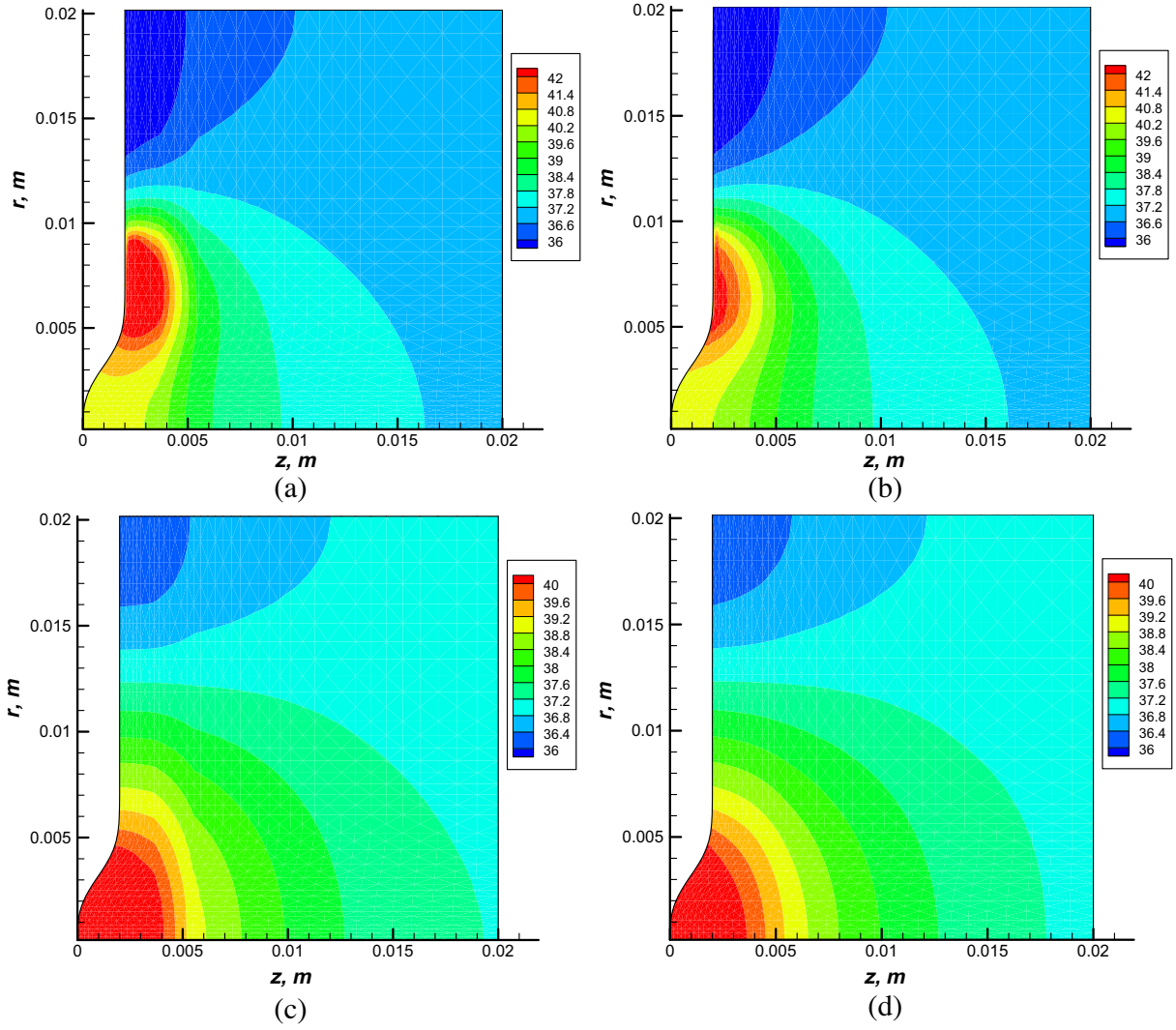

Fig. 7. Temperature field during thermal treatment by periodic laser irradiation according to regime 2 (Fig. 4). Calculations for the case of embedded gold nanoshells: a, b – at the peak of laser irradiation (at t = 35 min), c, d – before the next irradiation period (at t = 36.7 min); a, c – human tissue, b, d – arterial blood. The temperature is given in °C.

embed gold nanoshells into the human tissue around the tumor while using the suggested indirect heating strategy.

As was expected the computational results for the value of ξ_t (Fig. 6) indicate that tumor cells are not destroyed during the chosen soft treatment. As to the values of ξ_b, they are much less than ξ_t and possible conversions in blood do not lead to destruction of the cells.

Typical instantaneous temperature fields for the regime of comparatively slow heating ("2" in Fig. 4) with embedded gold nanoshells are presented in Fig. 7. The results for the tissue (Fig. 7a) and for arterial blood (Fig. 7b) are obtained at one of the peaks of laser irradiation (t = 35 min), while Fig. 7c and Fig. 7d show the temperatures of the tissue and arterial blood obtained before the next irradiation period (t = 36.7min). As can be expected, the temperature fields at the peak of irradiation exhibit a small overheating region close to the irradiated surface. The maximum temperature difference of tissue between this region and the center of the tumor is about 3.5 °C. Rather high temperatures in the tumor are reached due to thermal insulation of the tumor surface which allows conducted from irradiated surface heat to remain in the tumor and insignificant heat losses through the layer of fat which is characterized by a relatively low thermal conductivity. A small overheating of the circular superficial region around the tumor can be also helpful to isolate the tumor from healthy skin layers.

During non-heating period the heat is conducted towards the tumor so just before the next irradiation period (Fig. 7c, d) the tumor region becomes almost uniformly heated. From comparison of the local temperatures of tissue (Fig. 7a, c) and arterial blood (Fig. 7b, d) it can be seen that they are close to each other with the tissue temperature slightly increased due to lower absorption of radiation in blood. A local difference between the tissue and arterial blood in the overheated ring could reach 1.8 °C at the moment of the peak of irradiation. However, the temperature difference at the centre of the tumor is less than 0.5 °C. It should be noted that the temperature differences at the level of about one degree may be important for hyperthermia treatment.

The temperature fields for the same regime and at the same instants of time but for the case without embedded gold nanoshells are presented in Fig. 8. In general these temperature fields are very similar to those ones shown in Fig. 7. At the same time, the effect of the hot ring around the tumor is not so pronounced. So, one can use the gold nanoshells to reach this effect if necessary. As in the calculations with nanoshells, the temperature field in the tumor

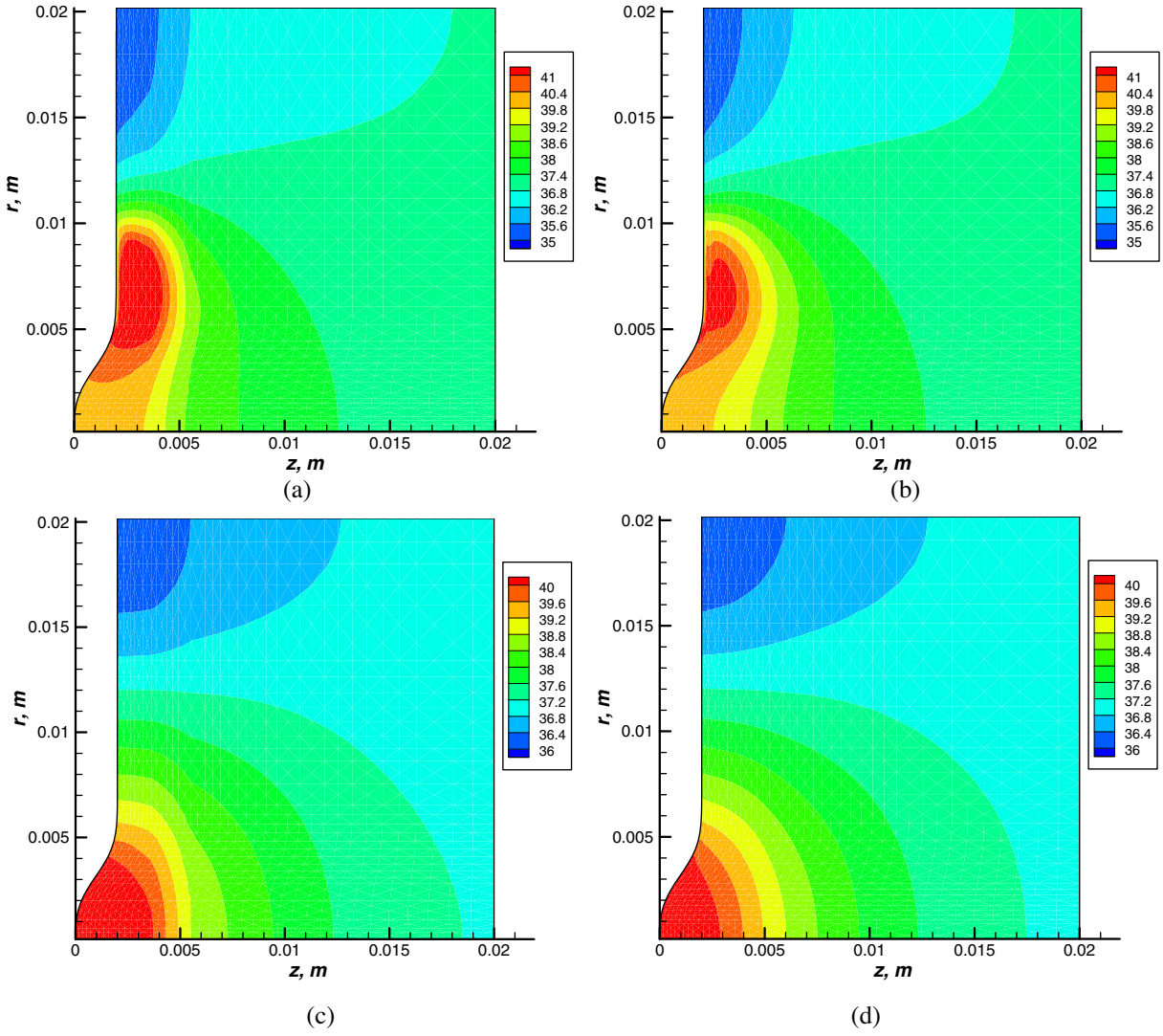

Fig. 8. Temperature field during thermal treatment by periodic laser irradiation according to regime 2 (Fig. 4). Calculations for the case without embedded gold nanoshells. Designations see in Fig. 7.

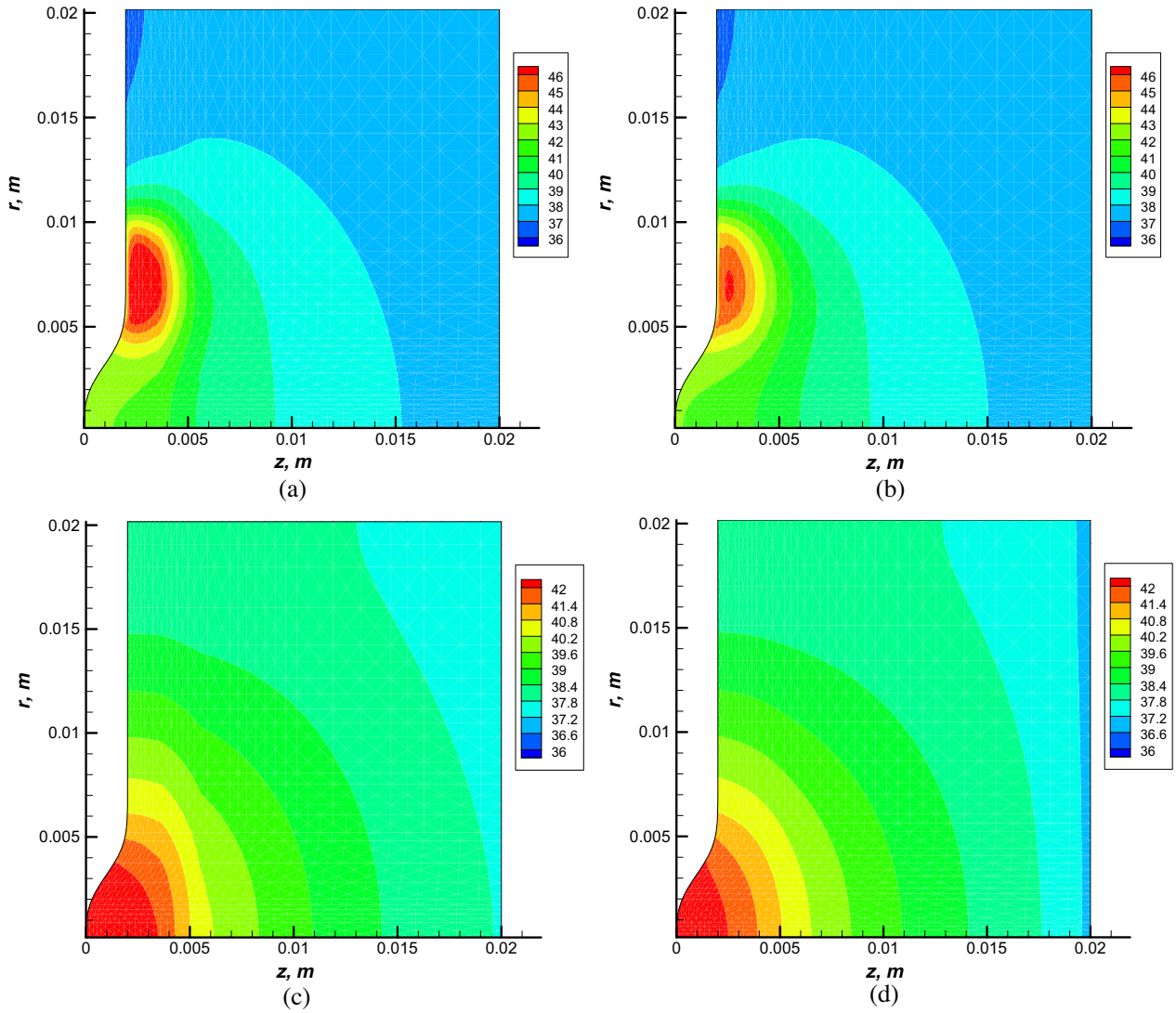

Fig. 9. Temperature field during thermal treatment by periodic laser irradiation according to regime 1 (Fig. 4). Calculations for the case without embedded gold nanoshells. Designations see in Fig. 7.

region is almost uniform. This supports the above statement that embedding of gold nanoshells around the tumor is not always necessary.

In order to compare the temperature fields for two heating regimes for the case without embedded gold nanoshells the results for faster heating regime ("1", Fig. 4) are presented in Fig. 9. As expected, the hot ring around the tumor is more prominent in this regime which means that this effect can be regulated by duration of the heating period. For both regimes the difference between the temperatures of tissue and blood is slightly less than in the case of embedded nanoshells.

Thus, in the case of a relatively slow laser-induced heating in the spectral range of low absorption of the radiation by blood, a simplified one-temperature model for approximate heat transfer calculations can be employed.

It should be noted that the proposed indirect heating strategy is more flexible as compared with the ordinary procedures because of many additional geometric and heat transfer parameters that can be used. Therefore, various required thermal regimes can be realized in medical practice. To our mind, a thermal model can be extended by a special analysis of the pain which depends not only on the local temperature level but also on the duration of heating period. Obviously, it is only one of possible further directions of studies based on the predicted transient temperature field in the body.

A validation of the developed computational model is an important task which is beyond the scope of the present paper. Most likely, the validation should be based mainly on temperature measurements (not only at the body surface but also at some selected points inside the tumor) [29].

5. Conclusions

A novel heating strategy for hyperthermia based on laser irradiation of the tissues surrounding a tumor is proposed and analyzed for the first time. The situations with and without gold nanoshells embedded in a human tissue are considered in detail. The proposed indirect heating strategy has some important advantages as compared with the ordinary direct laser irradiation of tumors: (1) the procedure is much more flexible due to additional parameters which enable to arrange more uniform heating and "choke" of the tumor laterally instead of the front heating, (2) one may be able to avoid or decrease undesirable local changes in arterial blood perfusion during soft thermal treatment, (3) the pain associated with

the procedure may be reduced by water cooling of the irradiated body surface and appropriate choice of irradiation parameters.

An advanced two-dimensional computational model for the indirect heating strategy has been developed. This model includes the laser radiation transfer in absorbing and anisotropically scattering tissues, the transient heat transfer in a human body taking into account the temperature difference between arterial blood and ambient tissues, and the kinetics of thermal damage of the tumor tissue cells.

An example problem for a superficial human cancer was solved numerically to understand a relative role of the problem parameters on the transient temperature field and to consider possible simplifications of the computational model. For a particular case of a prolonged soft thermal treatment of a superficial tumor, the temperature difference between arterial blood and ambient tissues appears to be insignificant, and the transient thermal state of the tumor can be approximately predicted on the basis of a one-temperature model. Further simplification of the computational model can be made due to very strong scattering of the laser radiation in superficial layers of the skin which allows the use of a one-dimensional solution for the radiative transfer problem.

Thermal calculations for a periodic laser irradiation showed that the required uniform heating of the tumor can be achieved for some superficial tumors even without gold nanoshells or other invasive procedures. This result may have important implications for medical practice.

Acknowledgements

The first author is grateful for the financial support of this work by CFD Laboratory, UNSW and Russian Foundation for Basic Research (grant no. 10-08-00218-a). The authors are also grateful to David Wong from Eastern Suburbs Dermatology, Sydney, for useful discussions.

References

[1] S. Lal, S.E. Clare, N.J. Halas, Nanoshell-enabled photothermal cancer therapy: Impending clinical impact, Accounts Chem. Res. 41 (12) (2008) 1842–1851.
[2] P. Cherukuri, S.A. Curley, Use of nanoparticles for targeted, noninvasive thermal destruction of malignant cells (Chapter 24), in: S.S. Grobmyer, B.B. Moudgil (Eds.), Cancer Nanotechnology, Springer, 2010, pp. 359–373.
[3] K. Cheng, S. Sun, Recent advances in syntheses and therapeutic applications of multifunctional porous hollow nanoparticles, Nano. Today 5 (3) (2010) 183–196.
[4] A.-R.A. Khaled, K. Vafai, The role of porous media in modeling flow and heat transfer in biological tissues, Int. J. Heat Mass Transfer 46 (26) (2003) 4989–5003.
[5] B. Khlebtsov, V. Zharov, A. Melnikov, V. Tuchin, N. Khlebtsov, Optical amplification of photothermal therapy with gold nanoparticles and nanoclusters, Nanotechnol. 17 (20, 28) (2006) 5167–5179.
[6] A. Nakayama, F. Kuwahara, A general bioheat transfer model based on the theory of porous media, Int. J. Heat Mass Transfer 51 (11–12) (2008) 3190–3199.
[7] N.G. Khlebtzov, L.A. Dykhman, Optical properties and biomedical applications of plasmonic nanoparticles, J. Quant. Spectr. Radiat. Transfer 111 (1) (2010) 1–35.
[8] X. Huang, M.A. El-Sayed, Gold nanoparticles: Optical properties and implementations in cancer diagnosis and photothermal therapy, J. Adv. Res. 1 (1) (2010) 13–28.
[9] J. Landry, P. Chréttien, D. Bernier, L.M. Nicole, N. Marceau, R.M. Tanguay, Thermotolerance and heat shock proteins induced by hyperthermia in rat liver cells, Int. J. Radiat. Oncol. Biol. Phys. 8 (1) (1982) 59–62.
[10] L.A. Dombrovsky, V. Timchenko, M. Jackson, G.H. Yeoh, A combined transient thermal model for laser hyperthermia of tumors with embedded gold nanoshells, Int. J. Heat Mass Transfer 54 (25–26) (2011) 5459–5469.
[11] J. Vera, Y. Bayazitoglu, Gold nanoshell density variation with laser power for induced hyperthermia, Int. J. Heat Mass Transfer 52 (3–4) (2009) 564–573.
[12] A. Szasz, G. Vincze, O. Szasz, B. Szasz, An energy analysis of extracellular hyperthermia, Electromagn. Bio. Med. 22 (2) (2003) 103–115.
[13] A. Szasz, G. Vincze, Dose concept of oncological hyperthermia: Heat-equation considering the cell destruction, J. Cancer Res. Therap. 2 (4) (2006) 171–181.
[14] M.H. Niemz, Laser-Tissue Interactions, Fundamentals and Applications, second ed., Biological and Medical Physics Series, Springer, Berlin, 2002.
[15] L.A. Dombrovsky, D. Baillis, Thermal Radiation in Disperse Systems: An Engineering Approach, Begell House, New York and Redding (CT), 2010.
[16] M.F. Modest, Radiative Heat Transfer, second ed., Academic Press, New York, 2003.
[17] J.R. Howell, R. Siegel, M.P. Mengüç, Thermal Radiation Heat Transfer, CRC Press, New York, 2010.
[18] L.A. Dombrovsky, D. Baillis, J.H. Randrianalisoa, Some physical models used to identify and analyze infrared radiative properties of semi-transparent dispersed materials, J. Spectr. Dynam. 1 (2011) (Paper 7).
[19] A. Fasano, D. Hömberg, D. Naumov, On a mathematical model for laser-induced thermotherapy, Appl. Math. Model. 34 (12) (2010) 3831–3840.
[20] S. Banerjee, S.K. Sharma, Use of Monte Carlo simulations for propagation of light in biomedical tissues, Appl. Opt. 49 (22) (2010) 4152–4159.
[21] L. Dombrovsky, W. Lipiński, A combined P_1 and Monte Carlo model for multi-dimensional radiative transfer problems in scattering media, Comput. Therm. Sci. 2 (6) (2010) 549–560.
[22] D. Yudovsky, A.J. Durkin, Hybrid diffusion and two-flux approximation for multilayered tissue light propagation modeling, Appl. Opt. 50 (21) (2011) 4237–4245.
[23] J. Mobley, T. Vo-Dinh, Optical properties of tissue, in: T. Vo-Dinh (Ed.), Biomedical Photonics Handbook, CRC Press, Boca Raton (FL), 2003. pp. 2-1–2-75.
[24] F.A. Duck, Physical Properties of Tissue: A Comprehensive Reference Book, Acad. Press, San Diego, 1990.
[25] W. Cheong, S.A. Prahl, A.J. Welsh, A review of the optical properties of biological tissues, IEEE J. Quant. Electron. 26 (12) (1990) 2166–2185.
[26] V.V. Tuchin, Tissue Optics: Light Scattering Methods and Instruments for Medical Diagnosis, second ed., vol. PM166, SPIE Press, Bellingham, WA, 2007.
[27] C.F. Bohren, D.R. Huffman, Absorption and Scattering of Light by Small Particles, Wiley, New York, 1983.
[28] M. Born, E. Wolf, Principles of Optics, seventh (expanded) ed., Cambridge Univ. Press, New York, 1999.
[29] Y. Feng, D. Fuentes, Model-based planning and real-time predictive control for laser-induced thermal therapy, Int. J. Hyperthermia 27 (8) (2011) 751–761.
[30] R.A. London, M.E. Glinsky, G.B. Zimmerman, D.S. Bailey, D.C. Eder, S.L. Jacques, Laser-tissue interaction modeling with LATIS, Appl. Optics 36 (34) (1997) 9068–9074.
[31] K. Peng, X. Gao, X. Qu, N. Ren, X. Chen, X. He, X. Wang, J. Liang, J. Tian, Graphics processing unit parallel accelerated solution of the discrete ordinates for photon transport in biological tissues, Appl. Optics 50 (21) (2011) 3808–3823.
[32] H.H. Pennes, Analysis of tissue and arterial blood temperature in the resting human forearm, J. Appl. Physiol. 1 (2) (1948) 93–122.
[33] T.J. Pfefer, B. Choi, G. Vargas, K.M. McNally, A.J. Welsh, Pulsed laser-induced thermal damage in whole blood, ASME J. Biomech. Eng. 122 (2) (2000) 196–202.
[34] W. Jia, G. Aguilar, W. Verkruysse, W. Franco, J.S. Nelson, Improvement of port wine stain laser therapy by skin preheating prior to cryogen spray cooling: a numerical simulation, Lasers Surg. Med. 38 (2) (2006) 155–162.
[35] L.A. Dombrovsky, E.P. Yukina, A.V. Kolpakov, V.A. Ivanov, Procedure for calculating the thermal destruction of phenolic carbon under the effect of intensive infrared radiation, High Temp. 4 (31) (1993) 566–572.
[36] B.V. Babu, A.S. Chaurasia, Modeling for pyrolysis of solid particle: kinetics and heat transfer effects, Energy Conv. Manag. 44 (14) (2003) 2251–2275.
[37] J.Z. Zhang, X.X. Zhang, M. Audette, A photothermal model of selective photothermolysis with dynamically changing vaporization temperature, Lasers Med. Sci. 26 (5) (2011) 630–640.
[38] F.C. Henriques, A.R. Moritz, Studies of thermal injury. I: The conduction of heat to and through skin and the temperatures attained therein. A theoretical and an experimental investigation, Am. J. Pathol. 23 (4) (1947) 530–549.
[39] A.R. Moritz, F.C. Henriques, Studies of thermal injury. II: The relative importance of time and surface temperature in the causation of cutaneous burns, Am. J. Pathol. 23 (5) (1947) 695–720.
[40] A. Bhattacharya, R.L. Mahajan, Temperature dependence of thermal conductivity of biological tissues, Physiol. Meas. 24 (3) (2003) 769–783.
[41] A.M.K. Nilsson, G.W. Lucassen, W. Verkruysse, S. Anderson-Engels, M.J.S. van Gemert, Changes in optical properties of human whole blood *in vitro* due to slow heating, Photochem. Photobiol. 65 (2) (1997) 366–373.
[42] A.M.K. Nilsson, C. Sturesson, D.L. Liu, S. Anderson-Engels, Changes in spectral shape of tissue optical properties in conjunction with laser-induced thermotherapy, Appl. Optics 37 (7) (1998) 1256–1267.
[43] M.P. Çetingül, C. Herman, A heat transfer model of skin tissue for the detection of lesions: sensitivity analysis, Phys. Medic. Biol. 55 (19) (2010) 5933–5951.
[44] M.P. Çetingül, C. Herman, Quantification of the thermal signature of a melanoma lesion, Int. J. Therm. Sci. 50 (4) (2011) 421–431.
[45] A.N. Bashkatov, E.A. Genina, V. Tuchin, Optical properties of skin, subcutaneous and muscle tissues: a review, J. Innovative Optical Health Sci. 4 (1) (2011) 9–38.
[46] H.-Q. Yang, Q.-Y. Lin, Z. Ye, S.-Q. Chen, S.-S. Xie, Finite element thermal analysis of breast with tumor and its comparison with thermography, in: X. Li, Q. Luo, Y. Gu (Eds.), Optics of Health Care and Biomedical Optics III, Proc. of SPIE, vol. 6826, 2007, 68260T-1. http://dx.doi.org/10.1117/12.756303.
[47] G.P. Peterson, C.H. Li, Heat and mass transfer in fluids with nanoparticle suspensions, Adv. Heat Transfer 39 (2006) 257–376.
[48] S.K. Das, S.U.S. Choi, W. Yu, T. Pradeep, Nanofluids: Science and Technology, Wiley, Hoboken, NJ, 2008.
[49] C. Nie, W.H. Marlow, Y.A. Hassan, Discussion of proposed mechanisms of thermal conductivity enhancement in nanofluids, Int. J. Heat Mass Transfer 51 (5–6) (2008) 1342–1348.

[50] M. Chandrasekhar, S. Suresh, A review on the mechanisms of heat transport in nanofluids, Heat Transfer Eng. 30 (14) (2009) 1136–1150.
[51] H.E. Patel, T. Sundararajan, S.K. Das, An experimental investigation into the thermal conductivity enhancement in oxide and metallic nanofluids, J. Nanopart. Res. 12 (3) (2010) 1015–1031.
[52] C. Kleinstreuer, Y. Feng, Experimental and theoretical studies of nanofluid thermal conductivity enhancement: a review, Nanoscale Res. Lett. 6 (1) (2011) 229.
[53] T.R. Gowrishankar, D.A. Stewart, G.T. Martin, J.C. Weaver, Transport lattice models of heat transport in skin with spatially heterogeneous, temperature dependent perfusion, BioMedical Eng. 3 (1) (2004) 42.
[54] K. Khanafer, J.L. Bull, I. Pop, R. Berguer, Influence of pulsative blood flow and heating scheme on the temperature distribution during hyperthermia treatment, Int. J. Heat Mass Transfer 50 (23–24) (2007) 4883–4890.
[55] V. Vuksanović, L.W. Sheppard, A. Stefanovska, Nonlinear relationship between level of blood flow and skin temperature for different dynamics of temperature change, Biophys. J. 94 (10) (2008) 78–80.
[56] I. Laakso, A. Hirata, Dominant factors affecting temperature rise in simulation of human thermoregulation during RF exposure, Phys. Med. Biol. 56 (23) (2011) 7449–7471.
[57] A. Boggan, M. Friebel, K. Dörschel, A. Hahn, G. Müller, Optical properties of circulating human blood in the wavelength range 400–2500 nm, J. Biol. Optics 4 (1) (1999) 36–46.
[58] M. Friebel, A. Roggan, G. Müller, M. Meinke, Determination of optical properties of human blood in the spectral range from 250 to 1100 nm using Monte Carlo simulations with hematocrit-dependent effective scattering phase functions, J. Biomed. Optics 11 (3) (2006) (paper 034021).
[59] M. Friebel, J. Helfmann, G. Müller, M. Meinke, Influence of shear rate on the optical properties of human blood in the spectral range 250 to 1100 nm, J. Biomed. Optics 12 (5) (2007) (paper 054005).
[60] M. Friebel, J. Helfmann, U. Netz, M. Meinke, Influence of oxygen saturation on the optical properties of human red blood cells in the spectral range 250 to 2000 nm, J. Biomed. Optics 14 (3) (2009) (paper 034001).
[61] W. Verkruysse, J.W. Pickering, J.F. Beek, M. Keijzer, M.J.C. van Gemert, Modeling the effect of wavelength on the pulsed dye laser treatment of port wine stains, Appl. Optics 32 (4) (1993) 393–398.
[62] W.J. Moressi, Mortality patterns of mouse sarcoma 180 cells resulting from direct heating and chronic microwave irradiation, Exper. Cell Res. 33 (1–2) (1964) 240–253.